Published in final edited form as:
J Mol Cell Cardiol. 2012 July ; 53(1): 15–23. doi:10.1016/j.yjmcc.2012.01.023.

Engraftment of human embryonic stem cell derived cardiomyocytes improves conduction in an arrhythmogenic in vitro model

Susan A. Thompson[a], **Paul W. Burridge**[b], **Elizabeth A. Lipke**[c], **Michael Shamblott**[d], **Elias T. Zambidis**[b], and **Leslie Tung**[a,*]

[a]Department of Biomedical Engineering, The Johns Hopkins University, Baltimore, MD, USA

[b]Institute for Cell Engineering and Division of Pediatric Oncology, Sidney Kimmel Comprehensive Cancer Center, The Johns Hopkins University, Baltimore, MD, USA

[c]Department of Chemical Engineering, Auburn University, Auburn, AL, USA

[d]Department of Neurology, The Johns Hopkins University and International Center for Spinal Cord Injury, Kennedy Krieger Institute, Baltimore, MD, USA

Abstract

In this study, we characterized the electrophysiological benefits of engrafting human embryonic stem cell-derived cardiomyocytes (hESC-CMs) in a model of arrhythmogenic cardiac tissue. Using transforming growth factor-β treated monolayers of neonatal rat ventricular cells (NRVCs), which retain several key aspects of the healing infarct such as an excess of contractile myofibroblasts and slowed, heterogeneous conduction, we assessed the ability of hESC-CMs to improve conduction and prevent arrhythmias. Cells from beating embryoid bodies (hESC-CMs) can form functional monolayers which beat spontaneously and can be electrically stimulated, with mean action potential duration of 275±36 ms and conduction velocity (CV) of 10.6±4.2 cm/s (n=3). These cells, or cells from non-beating embryoid bodies (hEBCs) were added to anisotropic, NRVC monolayers. Immunostaining demonstrated hESC-CM survival and engraftment, and dye transfer assays confirmed functional coupling between hESC-CMs and NRVCs. Conduction velocities significantly increased in anisotropic NRVC monolayers after engraftment of hESC-CMs (13.4±0.9 cm/s, n=35 vs. 30.1±3.2 cm/s, n=20 in the longitudinal direction and 4.3±0.3 cm/s vs. 9.3±0.9 cm/s in the transverse direction), but decreased to even lower values after engraftment of non-cardiac hEBCs (to 10.6±1.3 cm/s and 3.1± 0.5 cm/s, n=11, respectively). Furthermore, reentrant wave vulnerability in NRVC monolayers decreased by 20% after engraftment of hESC-CMs, but did not change with engraftment of hEBCs. Finally, the culture of hESC-CMs in transwell inserts, which prevents juxtacrine interactions, or engraftment with connexin43-silenced hESC-CMs provided no functional improvement to NRVC monolayers. These results demonstrate that hESC-CMs can reverse the slowing of conduction velocity, reduce the incidence of reentry, and augment impaired electrical propagation via gap junction coupling to host cardiomyocytes in this arrhythmogenic in vitro model.

*Corresponding author at: Department of Biomedical Engineering, The Johns Hopkins University, 720 Rutland Ave, Baltimore, MD 21205, USA. Tel.: +1 410 955 7453. ltung@jhu.edu (L. Tung).

Appendix A. Supplementary data

Supplementary data to this article can be found online at doi:10.1016/j.yjmcc.2012.01.023.

Disclosures

There are no potential conflicts of interest to disclose.

Keywords

Human embryonic stem cell; Electrophysiology; Arrhythmia; Cardiomyocytes; Myocardial infarction

1. Introduction

Heart disease is the most prevalent etiology of morbidity and mortality in the United States, and with a concurrent shortage of heart donors, there is a critical unmet need for new therapeutic approaches to restore injured myocardium. Following the acute injury of myocardial infarction, extensive wound healing initiates to salvage cardiac function. However, because native cardiomyocytes possess limited regenerative capacity, wound healing concludes with the net loss of ventricular muscle and the formation of a stable scar — a fibrotic, arrhythmogenic substrate [1]. Cardiac cell-based therapies have emerged as a promising therapeutic option following infarction [2], and many types of progenitors have been tested, including skeletal myoblasts, bone marrow-derived cells, mesenchymal stem cells, and resident cardiac stem cells [3]. However, most of these cell types have shown limited capacity to transdifferentiate into functional cardiomyocytes and/or electromechanically couple with existing myocardium [4,5].

Human embryonic stem cells (hESCs) are viable sources for cardiac therapeutics, since these pluripotent cells can generate unlimited numbers of electrophysiologically functional cardiomyocytes [4,6-8] that have the potential to electromechanically integrate into dysfunctional myocardium and improve cardiac function. Numerous studies have established the ability of human embryonic stem cell-derived cardiomyocytes (hESC-CMs) to improve myocardial function, suggesting possible roles of paracrine effects and/or direct myocardial regeneration [9-11].

To date, the results of in vivo studies examining the ability of hESC-CMs to improve cardiac function following myocardial infarction have been promising [9,12]. However, the number of incorporated cells attributed to the observed improvements has typically been low [12,13]. Furthermore, it is extremely challenging to obtain quantitative electrophysiological assessments following hESC-CM engraftment in vivo. These results underscore the need for studying the physiological mechanisms of cardiac cellular therapies in simpler, more defined, and more accessible systems. For example, our newly established arrhythmogenic in vitro model [14] is advantageous because it resembles a fibrotic, post-infarction environment in which the placement and density of hESC-CMs can be controlled, their viability can be monitored, and their experimental accessibility can be utilized. By using this arrhythmogenic in vitro model for hESC-CM engraftment, large numbers of pre-clinical experiments can be conducted using electrophysiological methods to study the complex mechanisms by which hESC-CMs can affect function in pathologic myocardium. Coupled with our recent advances in efficient hESC differentiation to cardiomyocytes [15], hESC-CMs can be generated in a scalable manner and electrophysiologically evaluated in vitro to create a large database on the mechanisms of functional improvement for future cardiac therapeutics.

It should also be noted that therapeutic benefit is currently defined primarily as improvement in mechanical function. Scant attention has been given to studying the ability of hESC-CMs to improve conduction and ameliorate the incidence of lethal arrhythmias such as ventricular fibrillation, a common cause of sudden cardiac death. We focused on this subject by utilizing our arrhythmogenic NRVC model [14] to delineate the electrophysiological benefits of hESC-CM engraftment. Using a combination of optical mapping and cellular

imaging, we tested the hypothesis that hESC-CMs can improve abnormal conduction and ameliorate arrhythmias in our model system.

2. Methods

An expanded Methods section is available in the online data supplement. Briefly, 20 mm diameter anisotropic monolayers of neonatal rat ventricular cells (NRVCs) were obtained by growing cells on parallel, 20 μm wide fibronectin lines separated by 10 μm spacing, formed by microcontact printing. All animal experiments were performed in accordance with guidelines set by the Johns Hopkins Committee on Animal Care and Use and were in compliance with all federal and state laws and regulations. Monolayers were treated with 5 ng/ml transforming growth factor-β (TGF-β) for 48–72 h to induce a fibrotic phenotype that served as control. Spontaneously beating embryoid bodies from the H9 (WA09) cell line were dissociated into hESC-CMs, and non-beating embryoid bodies were dissociated into human embryoid body cells (hEBCs). The use of the H9 cell line in these studies was evaluated and approved by the JHUSM Embryonic Stem Cell Research Oversight (ESCRO) Committee to assure that derivation and informed consent guidelines conformed to those recommended by the National Academy of Sciences for research involving hESCs. Both cell types were added to NRVC monolayers at a concentration of 100,000 per monolayer (Fig. 1). Three days later, hESC-CM supplemented monolayers and hEBC supplemented monolayers were immunostained for cardiac troponin I, connexin43 (Cx43), and human mitochondrial protein to visualize cellular engraftment. Troponin I and human mitochondrial protein positive cells were counted for purity of hESC-CMs and total cell number per monolayer was calculated. hESC-CMs and hEBCs were also preloaded in some experiments with calcein-AM before addition to NRVC monolayers to establish the presence of functional junctional coupling. Furthermore, the experimental groups were optically mapped with voltage-sensitive dye (10 μM di-4-ANEPPS) to determine the impact of engrafted hESC-CMs or hEBCs on conduction velocity (CV) in the longitudinal (LCV) and transverse (TCV) directions, action potential duration at 50% repolarization (APD_{50}), action potential duration at 80% repolarization (APD_{80}), conduction heterogeneity index (HI), incidence of reentrant waves, and pacing rate to initiate reentrant waves. In subsequent experiments, hESC-CMs or hEBCs were cultured in transwell inserts to prevent juxtacrine interactions with NRVC monolayers, and then monolayers were electrophysiologically characterized three days later. In some experiments hESC-CMs were transduced with Cx43 shRNA lentiviral particles for 7–8 h prior to engraftment to prevent electrical coupling to NRVCs. As a negative control, hESC-CMs were transduced with shRNA lentiviral particles encoding a scrambled shRNA sequence. The transduced hESC-CMs were engrafted on top of NRVC monolayers for subsequent electrophysiological analysis three days later, and Cx43 knockdown was confirmed using RT-PCR. Additionally, 200,000 hESC-CMs were plated onto 10 mm diameter areas coated with fibronectin and cultured for 3 weeks to create hESC-CM monolayers for subsequent optical mapping studies. For RT-PCR experiments, monolayers of hESC-CMs or hEBCs were cultured on fibronectin-coated coverslips for 3 days before extraction. Two-tail Student's t-tests were performed for independent data to determine statistically significant differences ($P<0.05$). All data are expressed as mean ±SEM.

3. Results

3.1. hESC differentiation generates electrophysiologically functional cardiomyocytes

Undifferentiated hESCs grown on mouse embryonic fibroblast (MEF) feeder layers (Fig. 2A) were differentiated into cardiomyocytes by first growing human embryoid bodies (hEBs) in suspension (Fig. 2B), and then allowing the hEBs to attach in order to identify and mark contracting hEBs (Fig. 2C). Labeled hEBs were mechanically dissected, enzymatically

dispersed into single cells, and plated to create large area monolayers of hESC-CMs that were functionally assessed by voltage mapping after approximately 3 weeks in culture and 50 days after the start of differentiation. All hESC-CM monolayers beat spontaneously and in synchrony. A time series of voltage maps (Figs. 2D–G) demonstrates that electrical wavefronts from a 1 Hz point stimulus propagate throughout the monolayer at an average velocity of 10.6±4.2 cm/s (n=3 monolayers). On average, hESC-CMs had action potentials with a mean APD_{80} of 275±36 ms and a mean APD_{50} of 182±33 ms (n=3 monolayers). Action potential traces (Fig. 2H) from 23 different recording sites show that there is considerable variation across the monolayer. Further, the coefficient of variation of APD_{80} (standard deviation divided by mean) is significantly higher in hESC-CM monolayers, 21±1%, n=3, than in NRVC monolayers, 12±1%, n=8, $p=10^{-4}$. Large areas of connected myocytes were present in the monolayer, as visualized by immunostaining for cardiac α-actinin and Cx43 (Fig. 2I). These experiments demonstrate that hESC-CMs are capable of forming an electrically functional syncytium.

3.2. hESC-CMs incorporate and functionally couple with NRVC monolayers

Although hESC-CM engraftment has been reported to be very low in previous in vivo infarction models [12,13], we found high survival and incorporation of hESC-CMs into our NRVC monolayers. We verified that dissociated hESC-CMs survive and engraft into NRVC monolayers by immunostaining monolayers for troponin I (blue) and human mitochondrial protein (green), and we confirmed that hESC-CMs (green and blue merge) interdigitate into the monolayer and interact with NRVCs laterally (Figs. 3A,C) and vertically in the z-plane (Figs. 3B,C). Furthermore, low magnification views demonstrate the relative distribution and density of engrafted hESC-CMs (red and green merge) after 3 days of co-culture (Fig. 3C). Image analysis showed that hESC-CMs comprised 78±4% of the stem cells added (n=10 monolayers), similar to purity percentages reported in our previous study [15]. Cell counts of 2–6 random fields of view showed that, because of continued proliferation, an estimated 192±38 thousand hESC-CMs (n=10 monolayers) were present in NRVC monolayers at the time of the mapping experiments, which on average contained an estimated 736±27 thousand host cardiomyocytes (n=17 monolayers).

After determining that hESC-CMs can integrate into NRVC monolayers, our next goal was to determine whether hESC-CMs functionally couple to NRVCs. Because heterocellular gap junctions between NRVCs and hESC-CMs were identified in both lateral and vertical directions (Figs. 3A,B), dye transfer experiments were performed by pre-loading hESC-CMs with 1 μM calcein-AM before adding them onto NRVC monolayers stained with Vybrant DiI solution (Supplemental Fig. 1). Host myofibroblasts were predominately found underneath the host cardiomyocytes in the NRVC monolayers [14] and were not in a position to interrupt the heterocellular coupling of hESC-CMs to the cardiomyocytes. HESC-CMs had extensive functional coupling with cardiomyocytes after 4 h, as demonstrated by the spread of calcein to the cardiomyocytes from calcein-loaded hESC-CMs. The same procedure was performed with hEBCs and also showed the spread of calcein, indicating that hEBC couple to NRVCs.

3.3. Engraftment of hESC-CMs improves conduction in NRVC monolayers

After functional coupling was demonstrated by dye transfer, the therapeutic potential of hESC-CMs was assessed by their effect on NRVC conduction at 2 Hz pacing, which is a pacing rate within the physiological range of human heart rates. As was previously shown, TGF-β treated monolayers (termed control monolayers) had slow conduction in comparison with untreated monolayers [14], both in the longitudinal (13.4±0.9 cm/s, n=35 vs. 29.9±1.2 cm/s, n=25, respectively) and transverse directions (4.3±0.3 cm/s vs. 10.2± 0.4 cm/s, respectively). The addition of hESC-CMs to control monolayers significantly improved

conduction velocity (to 30.1±3.2 cm/s in the longitudinal direction and 9.3±0.9 cm/s in the transverse direction, n=20, Figs. 4A–C). However, the addition of hEBCs (dissociated from non-contracting hEBs subjected to the same differentiation protocol) to control monolayers did not improve conduction, and even decreased CV further (to 10.6±1.3 cm/s in the longitudinal direction and 3.1±0.5 cm/s in the transverse direction, n=11, Figs. 4A–C). The hEBCs' inability to improve conduction in NRVC monolayers may result from their lowered expression of sodium channels (SCN5a), Cx43 (GJA1), or inward rectifying potassium channels (KCNJ2) compared with hESC-CMs (Fig. 4D). Subsequent staining of monolayers supplemented with hEBCs for human mitochondrial protein and cardiac troponin I showed extensive survival of hEBCs, but no positive staining for cardiac troponin I (not shown). Therefore, functional cardiomyocytes derived from beating EBs appear to be necessary and sufficient for improving conduction velocity in control monolayers.

3.4. Engrafted hESC-CMs reduce the vulnerability to arrhythmia in NRVC monolayers

Because the addition of hESC-CMs to control monolayers significantly improved CV, we also tested whether engrafted hESC-CMs had an effect on the arrhythmic vulnerability of the monolayers, as one might expect given that the wavelength of the propagating wave, which is estimated as the product of CV and APD, is an important factor in arrhythmogenesis [16]. In addition to slowed conduction, control monolayers displayed both a high incidence of reentrant (spiral) waves (93%, n=47) and a low pacing rate to initiate reentrant waves (3.5±0.1 Hz, n=35, Fig. 5). The addition of hESC-CMs to control monolayers (n=20) significantly decreased the incidence of reentrant waves by 20% (to 73%, n=15, p=0.05), and increased the pacing rate to initiate reentrant waves by 1 Hz (to 4.5±0.2 Hz, n=11, p=0.02, Fig. 5). On the other hand, engraftment of hEBCs had no effect on either the incidence of reentrant waves (90%, n=10) or the initiating pacing rate (3.8±0.3 Hz, n=9, Fig. 5) of control monolayers.

We then investigated whether hESC-CMs had an effect on APD_{80}, given that wavelength also depends on this parameter. The addition of hESC-CMs to control monolayers had no significant effect on APD_{80} (175±3 ms, n=44 for control monolayers vs. 173±5 ms for hESC-CM supplemented monolayers, n=20). On the other hand, the addition of hEBCs to control monolayers prolonged APD_{80} (to 188±7 ms, n=11, p=0.05), but not enough to reduce the high incidence of arrhythmias.

Finally, we quantified the heterogeneity of conduction, a condition that promotes the initiation of reentry. Neither the addition of hESC-CMs (1.7±0.1, n=20, p=0.9) or hEBCs (1.8±0.2, n=11, p=0.5) had a significant effect on HI of control monolayers (1.7±0.1, n=32). To summarize, hESC-CMs, but not hEBCs, were capable of decreasing the high incidence of reentrant waves in NRVC monolayers and increasing their initiating pacing rate.

3.5. Direct cellular contact between hESC-CMs and host cardiomyocytes is necessary for functional improvement

To test the possibility that hESC-CMs may improve conduction in NRVC monolayers through the release of paracrine factors, hESC-CMs were co-cultured in transwell inserts next to, but not contacting NRVCs. Both the isochrone maps (20 ms spacing, Fig. 6A) and summary plots of LCV and TCV (Figs. 6B and C, respectively) show that while direct addition of hESC-CMs significantly elevated LCV and TCV in control monolayers, hESC-CMs cultured in transwell inserts had no significant effect on either velocity (15.0±3.7 cm/s and 2.7±0.7 cm/s, n=5, respectively). Furthermore, the addition of hESC-CMs in transwell inserts to control monolayers did not significantly change the incidence of reentrant waves (80%, n=5) or initiating pacing rate (3.3±0.3 Hz, n=4). Likewise, the addition of hEBCs in transwell inserts did not significantly affect LCV (Fig. 6B), TCV (Fig. 6C), the incidence of

reentrant waves, or the initiating pacing rate (16.7±4.2 cm/s, 2.9±0.7 cm/s, 100%, and 3.3±0.3 Hz, n=4, respectively). Consequently, these studies show that juxtacrine interactions between hESC-CMs and cardiomyocytes within the monolayers, and not paracrine interactions alone, are required to produce functional improvements in conduction.

3.6. Engraftment of Cx43 shRNA hESC-CMs does not improve conduction in NRVC monolayers

Because Cx43 is the most abundantly expressed gap junction protein in our dissociated hESC-CMs, we conducted gene silencing experiments with Cx43 shRNA to observe the consequences of preventing electrical coupling of hESC-CMs to cardiomyocytes within NRVC monolayers. LCV (Fig. 7A) and TCV (Fig. 7B) plots show that while control (scrambled) shRNA hESC-CMs were able to significantly restore conduction after engraftment in control monolayers (28.1±5.4 cm/s and 5.9±0.8 cm/s, n=4, respectively), engraftment of Cx43 shRNA hESC-CMs had no effect on LCV or TCV (15.7±2.6 cm/s and 3.8±0.9 cm/s, n=7, respectively). Furthermore, engraftment of Cx43 shRNA hESC-CMs did not decrease the incidence of reentrant waves (100%, n=7), or increase the low initiating pacing rate of 4.1±0.2 Hz, n=7 in control monolayers (4.7±0.2 Hz, n=7, p=0.2). Real time RT-PCR confirmed that Cx43 shRNA transduction decreased Cx43 mRNA expression by 88±12% compared with that in control shRNA hESC-CMs (p=0.002, n=3). An immunostain image of Cx43 shRNA hESC-CMs (troponin I (blue) and human mitochondrial protein (green)) engrafted into a NRVC monolayer shows that Cx43 shRNA hESC-CMs were present, yet did not appear to express Cx43 (red, Fig. 7C). Therefore, electrical coupling between hESC-CMs and host myocytes in NRVC monolayers appears to be a prerequisite for functional improvements in conduction.

4. Discussion

Cardiac regenerative medicine aims to restore lost myocardial function by using cellular treatments, and various cell-based clinical trials are already underway [3]. Stem cell based therapies are particularly attractive in cardiology because pluripotent stem cells can generate large numbers of cardiomyocytes capable of electromechanical integration into host tissue. After engraftment of hESC-CMs into myocardial infarcts, improvement in global mechanical function has been reported in several animal studies [9,12,17]. However, these studies also highlight the lack of knowledge concerning the role of hESC-CMs in electrophysiological improvement. In this study, we investigated the electrophysiological impact of hESC-CMs engrafted into an arrhythmogenic in vitro model, using optical mapping to assess the benefits of engraftment on wavefront propagation and vulnerability to reentrant arrhythmia.

Because reentry is responsible for approximately 85% of arrhythmias initiated after ischemia and infarction [18], and current therapies offer incomplete relief, there is high demand for reliable treatments to reduce episodes of reentry. Implantable defibrillators are currently the only reliable treatment option to prevent an episode of ventricular fibrillation from becoming fatal, but they represent a retrospective therapy that does not address the underlying tissue substrate. In conjunction with defibrillators, current antiarrhythmic therapies focus on further depressing (with pharmacological agents) and/or blocking (with ablation) local conduction in order to prevent or terminate reentry, but these interventions often exacerbate the incidence of arrhythmias. However, it has been shown that reentry can be prevented if the waveform conducts through the arrhythmogenic tissue at an enhanced velocity (as opposed to the slowed conduction often observed) [19]. While there are no pharmacologic therapies currently in clinical use that improve cardiac conduction, investigative studies that employ gap junction enhancers have begun [20]. Similarly, the use of hESC-CM cell therapy to enhance conduction represents a novel and alternative

antiarrhythmic strategy that we show has potential to reduce life threatening cardiac conditions.

Although in vivo studies are necessary for clinical approval, one limitation of such studies is that the relatively small numbers of animals used preclude the collection of a large dataset for thorough assessment of the electrophysiological incorporation of hESC-CMs. An in vitro model of engraftment allows thorough investigation of hESC-CM electrophysiology following incorporation with host myocytes, and can be used in future studies to help anticipate how the engraftment outcome might change with different engraftment strategies (e.g. cardiac progenitor cell type, cell densities and distributions, multi-cell composition, media, growth factors, survival cocktails, etc.), greatly enhancing the speed at which progress towards the use of cell therapies can be made.

Our experimental in vitro model is advantageous because it allows quantification of the electrophysiological benefits of hESC-CMs without the full complexity and variability of the in vivo environment. The longitudinally-patterned myocytes and adjacent contractile myofibroblasts treated with TGF-β retain several key aspects of the microenvironment of a healing infarct, such as slowed, heterogeneous conduction in comparison with untreated monolayers. We previously proposed that through mechanical coupling between myofibroblasts and cardiomyocytes, myofibroblast contraction may activate mechanosensitive channels that depolarize the cardiomyocyte membrane, thereby inactivating the sodium channels that drive conduction [14].

Recent studies have shown that hESC-CMs mature over time in culture to a more adult phenotype [21], have local control of excitation–contraction coupling [8], are generally of the ventricular subtype [22], and can possess adult-like AP upstroke velocities (150 V/s) and maximum diastolic potentials (−80 mV) [6]. Furthermore, hESC-CMs express connexins [23], form gap junctions with neonatal rat ventricular myocytes [24], and produce synchronous contractions with neonatal rat ventricular myocytes [25]. Thus, cardiomyocytes derived from hESCs are capable of electrical coupling to myocytes and bridging between functionally separated myocytes.

Additionally, because the slowing of conduction in our NRVC monolayers may arise from myofibroblast-induced depolarization of native cardiomyocytes [14], hESC-CMs that are electrically coupled to the host cardiomyocytes may improve conduction by hyperpolarizing the host's (depolarized) resting potential, thereby increasing sodium channel availability and cell excitability. Electrically coupled hESC-CMs may also improve conduction by contributing inward sodium current, which is large enough to drive propagation in hESC-CM-only monolayers (Fig. 2). Because hESC-CMs express robust sodium channels with kinetics similar to adult sodium channels, but with activation shifted approximately 15 mV in the depolarized direction [22], they can contribute excitatory current at the depolarized resting potentials presumed to be present in NRVC monolayers. Similarly, it has been shown that transducing skeletal muscle sodium channels (which operate more effectively at depolarized potentials) into epicardial infarct border zones increases the maximum upstroke velocity and reduces the incidence of arrhythmias [26]. In contrast, the failure of hEBCs to improve conduction velocity may be attributed to the less negative resting potentials found in non-excitable cells [27], or low expression of sodium channels, inward rectifying potassium channels, and Cx43 (Fig. 4). It may be for similar reasons that engraftment of skeletal myoblasts, bone marrow cells or cardiac myofibroblasts to mouse infarct areas was found to exert no therapeutic benefit [28]. In summary, we conclude that the improvement in conduction brought about by the addition of hESC-CMs to NRVC monolayers likely arises from their electrical coupling to the resident cardiomyocytes, their ability to act as short

range electrical bridges, their hyperpolarizing effect on the cardiomyocytes which increases sodium current availability, and their contribution of exogenous sodium current.

We also predict that the beneficial effects of hESC-CM engraftment have the potential to improve over time. Although the initial seeding ratio of hESC-CMs to the host myocytes in the monolayer was approximately 1:10, hESC-CMs still possessed substantial proliferative potential, and in our model, the hESC-CM:NRVC ratio increased to 1:4, with some local areas having near 1:2 hESC-CM:host myocyte ratio, after only 3 days in culture. One study reported that 4 weeks after hESC-CMs transplantation into a rat heart, the graft expanded seven-fold [29]. A high fraction of hESC-CMs increases the likelihood that hESC-CMs can improve conduction through electrical coupling.

Existing in vivo data for the engraftment of hESC-CMs has demonstrated that these cells can survive and mature in the rat heart and enhance myocardial function following acute myocardial infarction, e.g. preserve fractional shortening and attenuate the course of ventricular remodeling [9,11,12]. However, because of the transient functional improvement observed, these studies speculated that the improvement is most likely due to paracrine contributions of the hESC-CMs. To test the possibility that hESC-CMs may also improve conduction by secreting paracrine factors after 3 days in culture, paracrine signaling was studied using transwell inserts that prevent direct cellular coupling. HESC-CMs cultured in transwell inserts did not improve conduction in NRVC monolayers (Fig. 6), unlike those that could directly couple to the cardiomyocytes (Figs. 4, 5). This result indicated that juxtacrine interactions between hESC-CMs and cells in the NRVC monolayers are required to produce an improvement in electrical propagation and are consistent with a heterocellular coupling effect. Our results do not rule out the possibility that longer co-culture times may result in a significant paracrine effect.

Finally, we observed a significant decrease in the incidence of reentrant waves after the engraftment of hESC-CMs in NRVC monolayers (Fig. 5), but not with hEBC engraftment, hESC-CM addition to transwell inserts, or engraftment of Cx43 shRNA hESC-CMs. This result is consistent with the results of a previous study, which demonstrated that engraftment of either embryonic cardiomyocytes or skeletal myoblasts from the mouse engineered to express Cx43 reduced the incidence of ventricular tachycardia in a mouse myocardial infarct model [28]. A decrease in the incidence rate can arise from a decrease in heterogeneity of conduction [30] or an increase in the wavelength of the propagating wave, estimated as the product of CV and APD [16]. HESC-CMs had little effect on HI or APD_{80}, but profoundly increased CV. The mechanism by which the incidence of reentrant waves decreases cannot be from the contribution of hESC-CM sodium current because the rate (4–5 Hz) is significantly higher than the maximum frequency at which conduction can be supported by hESC-CMs alone (Fig. 2). However, hESC-CMs can still effectively lower the resting potential of the host myocytes and reduce the incidence of reentrant waves as described earlier. Such a mechanism for therapeutic benefit of hESC-CMs at high pacing rates may translate to humans, in which heart rates can reach 270 beats per minute (4.5 Hz) during tachycardia [31]. Although a recent study did show that mouse embryonic stem cell-derived cardiomyocyte transplantation into infracted myocardium was associated with a significantly higher prevalence of inducible ventricular tacharrhythmias than transplantation with undifferentiated embryonic stem cells [32], similar studies need to be repeated with hESC-CMs for clinical relevance, since it is well accepted that knowledge derived from mouse embryonic stem cells often is not directly translatable to hESCs [33]. Finally, while some stem cell types can induce cardiac arrhythmias, which has led to increased patient morbidity and mortality in clinical trials [34], our results suggest that hESC-CMs can reduce the likelihood of reentrant arrhythmias under certain conditions such as post-infarct fibrosis.

Our results are specific to the in vitro conditions of our model, and it remains to be seen whether they extrapolate clinically in vivo. Our cells are maintained under culture conditions (culture media, 2D rigid substrate, lack of hemodynamic loading), which can affect cell shape, protein expression and cell function [35]. Also, we used the H9 cell line under two differentiation protocols, and although we did not observe a difference in the results depending on the protocol, our results may vary with cardiomyocytes derived using other differentiation protocols. If our findings are confirmed with multiple pluripotent stem cell lines and in large animal in vivo studies, these differentiated cells may provide a means to reduce the incidence of clinically relevant reentrant arrhythmias.

5. Conclusion

The results of our study demonstrate that hESC-CMs improve conduction in our NRVC arrhythmogenic model through electrical coupling to host myocytes and subsequent restoration of electrical conduction of propagating wavefronts. We found that hESC-CMs are autonomously capable of forming electrophysiologically functional, macroscale, multicellular monolayers, and that dissociated cells could survive and engraft into NRVC monolayers. Furthermore, hESC-CMs functionally couple to host myocytes, dramatically improve the speed of conduction, decrease the vulnerability to reentrant arrhythmias, and increase the beat rate required to produce arrhythmias. In contrast, differentiated, non-beating hEBCs, or Cx43-silenced hESC-CMs, do not produce these functional benefits. Finally, juxtacrine interactions between hESC-CMs and host cardiomyocytes appear to be necessary for conduction improvement.

Supplementary Material

Refer to Web version on PubMed Central for supplementary material.

Acknowledgments

We are grateful to Lior Gepstein for generously training E.A.L. in his laboratory on the methods for culturing and differentiating human embryonic stem cells.

Funding for this work was provided by a grant from the Joint Technion-Hopkins Program for the Biomedical Sciences and Biomedical Engineering (L.T.), grants from the Maryland Stem Cell Research Fund 2008-MSCRFE-0084-00 (L.T.), 2011-MSCRFII-0008-00 (ETZ) and 2008-MSCRFII-0379-00 (ETZ), NIH grants R01-HL066239 (L.T.), U01HL099775 and U01HL100397 (ETZ), Maryland Stem Cell Research Fund Fellowship (P.W.B.), and a National Science Foundation *Integrative Graduate Education and Research Traineeship* (S.A.T.).

References

1. van den Borne SWM, Diez J, Blankesteijn WM, Verjans J, Hofstra L, Narula J. Myocardial remodeling after infarction: the role of myofibroblasts. Nat Rev Cardiol. 2010; 7(1):30–7. [PubMed: 19949426]
2. Fukuda K, Yuasa S. Stem cells as a source of regenerative cardiomyocytes. Circ Res. 2006; 98(8): 1002–13. [PubMed: 16645150]
3. Soejitno A, Wihandani DM, Kuswardhani RA. Clinical applications of stem cell therapy for regenerating the heart. Acta Med Indones. 2010; 42(4):243–57. [PubMed: 21063047]
4. Guan K, Hasenfuss G. Do stem cells in the heart truly differentiate into cardiomyocytes? J Mol Cell Cardiol. 2007; 43(4):377–87. [PubMed: 17716688]
5. Menasche P. Cardiac cell therapy: lessons from clinical trials. J Mol Cell Cardiol. 2011; 50(2):258–65. [PubMed: 20600097]
6. Pekkanen-Mattila M, Chapman H, Kerkela E, Suuronen R, Skottman H, Koivisto AP, et al. Human embryonic stem cell-derived cardiomyocytes: demonstration of a portion of cardiac cells with fairly mature electrical phenotype. Exp Biol Med. 2010; 235(4):522–30.

7. Zeevi-Levin N, Fau - Itskovitz-Eldor J, Itskovitz-Eldor J, Fau - Binah O, Binah O. Functional properties of human embryonic stem cell-derived cardiomyocytes. Crit Rev Eukaryot Gene Expr. 2010; 20(1):51–9. [PubMed: 20528737]
8. Zhu WZ, Santana LF, Laflamme MA. Local control of excitation-contraction coupling in human embryonic stem cell-derived cardiomyocytes. PLoS One. 2009; 4(4):e5407. [PubMed: 19404384]
9. Caspi O, Huber I, Kehat I, Habib M, Arbel G, Gepstein A, et al. Transplantation of human embryonic stem cell-derived cardiomyocytes improves myocardial performance in infarcted rat hearts. J Am Coll Cardiol. 2007; 50(19):1884–93. [PubMed: 17980256]
10. Dai W, Field LJ, Rubart M, Reuter S, Hale SL, Zweigerdt R, et al. Survival and maturation of human embryonic stem cell-derived cardiomyocytes in rat hearts. J Mol Cell Cardiol. 2007; 43(4): 504–16. [PubMed: 17707399]
11. van Laake LW, Passier R, Doevendans PA, Mummery CL. Human embryonic stem cell-derived cardiomyocytes and cardiac repair in rodents. Circ Res. 2008; 102(9):1008–10. [PubMed: 18436793]
12. Laflamme MA, Chen KY, Naumova AV, Muskheli V, Fugate JA, Dupras SK, et al. Cardiomyocytes derived from human embryonic stem cells in pro-survival factors enhance function of infarcted rat hearts. Nat Biotechnol. 2007; 25(9):1015–24. [PubMed: 17721512]
13. Leor J, Gerecht S, Cohen S, Miller L, Holbova R, Ziskind A, et al. Human embryonic stem cell transplantation to repair the infarcted myocardium. Heart. 2007; 93(10):1278–84. [PubMed: 17566061]
14. Thompson SA, Copeland CR, Reich DH, Tung L. Mechanical coupling between myofibroblasts and cardiomyocytes slows electric conduction in fibrotic cell monolayers. Circulation. 2011; 123(19):2083–93. [PubMed: 21537003]
15. Burridge PW, Thompson S, Millrod MA, Weinberg S, Yuan X, Peters A, et al. A universal system for highly efficient cardiac differentiation of human induced pluripotent stem cells that eliminates interline variability. PLoS One. 2011; 6(4):e18293. [PubMed: 21494607]
16. Tung, L.; Bursac, N.; Aguel, F. Rotors and spiral waves in two dimensions. In: Zipes, DP.; Jalife, J., editors. Cardiac electrophysiology — from cell to bedside. Philadelphia, PA: W. B. Saunders; 2004. p. 336-44.
17. Tomescot A, Leschik J, Bellamy V, Dubois G, Messas E, Bruneval P, et al. Differentiation in vivo of cardiac committed human embryonic stem cells in postmyocardial infarcted rats. Stem Cells. 2007; 25(9):2200–5. [PubMed: 17540853]
18. Wit AL, Janse MJ. Experimental models of ventricular tachycardia and fibrillation caused by ischemia and infarction. Circulation. 1992; 85(1):I32–42. [PubMed: 1728503]
19. Pamintuan JC, Dreifus LS, Watanabe Y. Comparative mechanisms of antiarrhythmic agents. Am J Cardiol. 1970; 26(5):512–9. [PubMed: 5478839]
20. Rossman EI, Liu K, Morgan GA, Swillo RE, Krueger JA, Gardell SJ, et al. The gap junction modifier, GAP-134 [(2*S*,4R)-1-(2-aminoacetyl)-4-benzamido-pyrrolidine-2-carboxylic acid], improves conduction and reduces atrial fibrillation/flutter in the canine sterile pericarditis model. J Pharmacol Exp Ther. 2009; 329(3):1127–33. [PubMed: 19252062]
21. Sartiani L, Bettiol E, Stillitano F, Mugelli A, Cerbai E, Jaconi ME. Developmental changes in cardiomyocytes differentiated from human embryonic stem cells: a molecular and electrophysiological approach. Stem Cells. 2007; 25(5):1136–44. [PubMed: 17255522]
22. Satin J, Kehat I, Caspi O, Huber I, Arbel G, Itzhaki I, et al. Mechanism of spontaneous excitability in human embryonic stem cell derived cardiomyocytes. J Physiol. 2004; 559(2):479–96. [PubMed: 15243138]
23. Kehat I, Gepstein A, Spira A, Itskovitz-Eldor J, Gepstein L. High-resolution electrophysiological assessment of human embryonic stem cell-derived cardiomyocytes: a novel in vitro model for the study of conduction. Circ Res. 2002; 91(8):659–61. [PubMed: 12386141]
24. Kehat I, Khimovich L, Caspi O, Gepstein A, Shofti R, Arbel G, et al. Electromechanical integration of cardiomyocytes derived from human embryonic stem cells. Nat Biotechnol. 2004; 22(10):1282–9. [PubMed: 15448703]
25. Xue T, Cho HC, Akar FG, Tsang S-Y, Jones SP, Marban E, et al. Functional integration of electrically active cardiac derivatives from genetically engineered human embryonic stem cells

with quiescent recipient ventricular cardiomyocytes: insights into the development of cell-based pacemakers. Circulation. 2005; 111(1):11–20. [PubMed: 15611367]

26. Lau DH, Clausen C, Sosunov EA, Shlapakova IN, Anyukhovsky EP, Danilo P Jr, et al. Epicardial border zone overexpression of skeletal muscle sodium channel SkM1 normalizes activation, preserves conduction, and suppresses ventricular arrhythmia: an in silico, in vivo, in vitro study. Circulation. 2009; 119(1):19–27. [PubMed: 19103989]
27. Williams JA. Origin of transmembrane potentials in non-excitable cells. J Theor Biol. 1970; 28(2): 287–96. [PubMed: 5487645]
28. Roell W, Lewalter T, Sasse P, Tallini YN, Choi B-R, Breitbach M, et al. Engraftment of connexin 43-expressing cells prevents post-infarct arrhythmia. Nature. 2007; 450(7171):819–24. [PubMed: 18064002]
29. Laflamme MA, Gold J, Xu C, Hassanipour M, Rosler E, Police S, et al. Formation of human myocardium in the rat heart from human embryonic stem cells. Am J Pathol. 2005; 167(3):663–71. [PubMed: 16127147]
30. Hayashi H, Terada H, McDonald T. Arrhythmia and electrical heterogeneity during prolonged hypoxia in guinea pig papillary muscles. Can J Physiol Pharmacol. 1997; 75(1):44–51. [PubMed: 9101064]
31. Dobmeyer DJ, Stine RA, Leier CV, Greenberg R, Schaal SF. The arrhythmogenic effects of caffeine in human beings. N Engl J Med. 1983; 308(14):814–6. [PubMed: 6835272]
32. Liao S-Y, Liu Y, Siu C-W, Zhang Y, Lai W-H, Au K-W, et al. Proarrhythmic risk of embryonic stem cell-derived cardiomyocyte transplantation in infarcted myocardium. Heart Rhythm. 2010; 7(12):1852–9. [PubMed: 20833268]
33. Laflamme MA, Murry CE. Regenerating the heart. Nat Biotechnol. 2005; 23(7):845–56. [PubMed: 16003373]
34. Oettgen P. Cardiac stem cell therapy. Circulation. 2006; 114(4):353–8. [PubMed: 16864740]
35. Tung, L.; Thompson, S. Advantages and pitfalls of cell cultures as model systems to study cardiac mechanoelectric coupling. In: Kohl, P.; Sachs, F.; Franz, MR., editors. Cardiac mechano-electric coupling and arrhythmias. Oxford, U.K.: Oxford University Press; 2011. p. 143-50.

Glossary

hEBCs	human embryoid body derived cells
NRVCs	neonatal rat ventricular cells
CV	conduction velocity
LCV	longitudinal CV
TCV	transverse CV
APD_{50}	action potential duration at 50% repolarization
APD_{80}	action potential duration at 80% repolarization
HI	conduction heterogeneity index

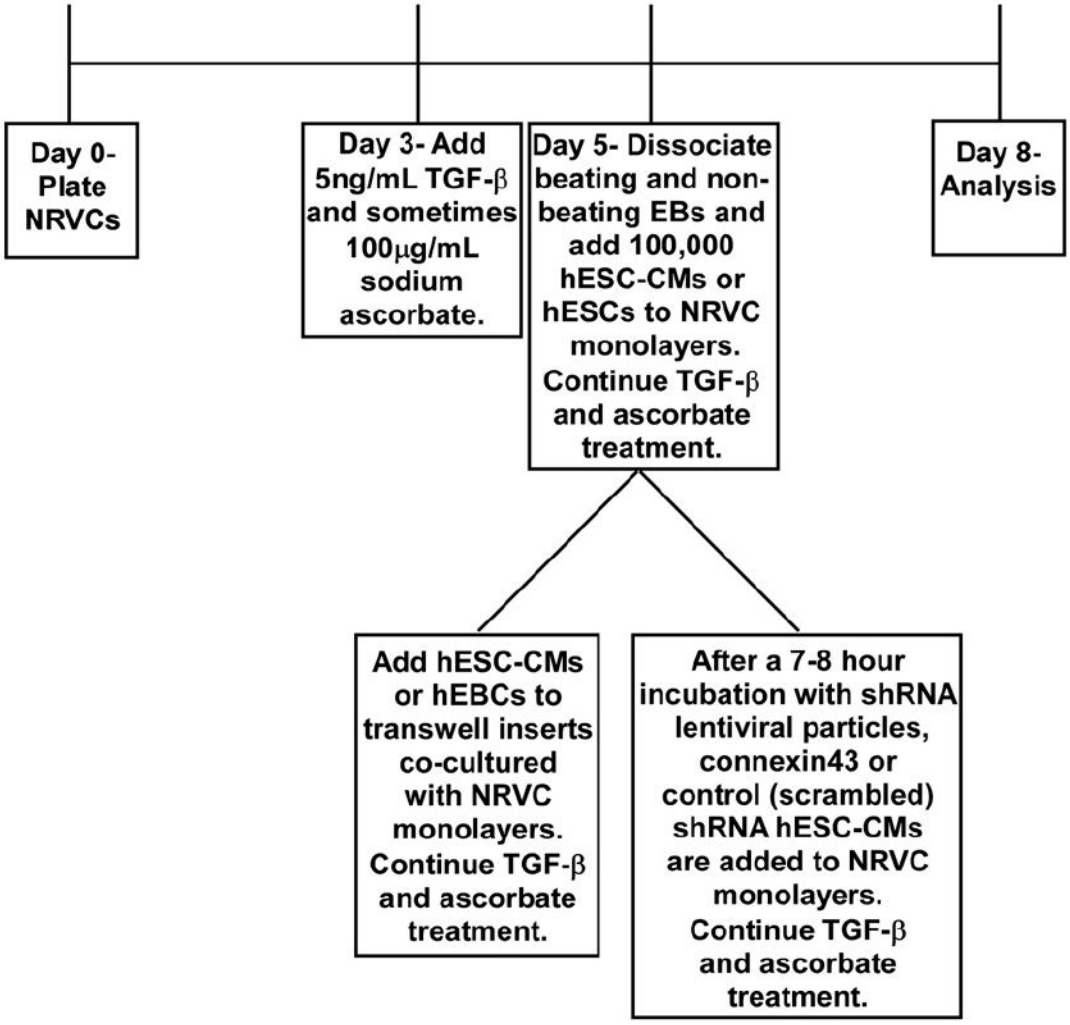

Fig. 1.
Timeline for cell culture: creation of arrhythmogenic NRVC monolayers and subsequent addition of hESC-CMs or hEBCs.

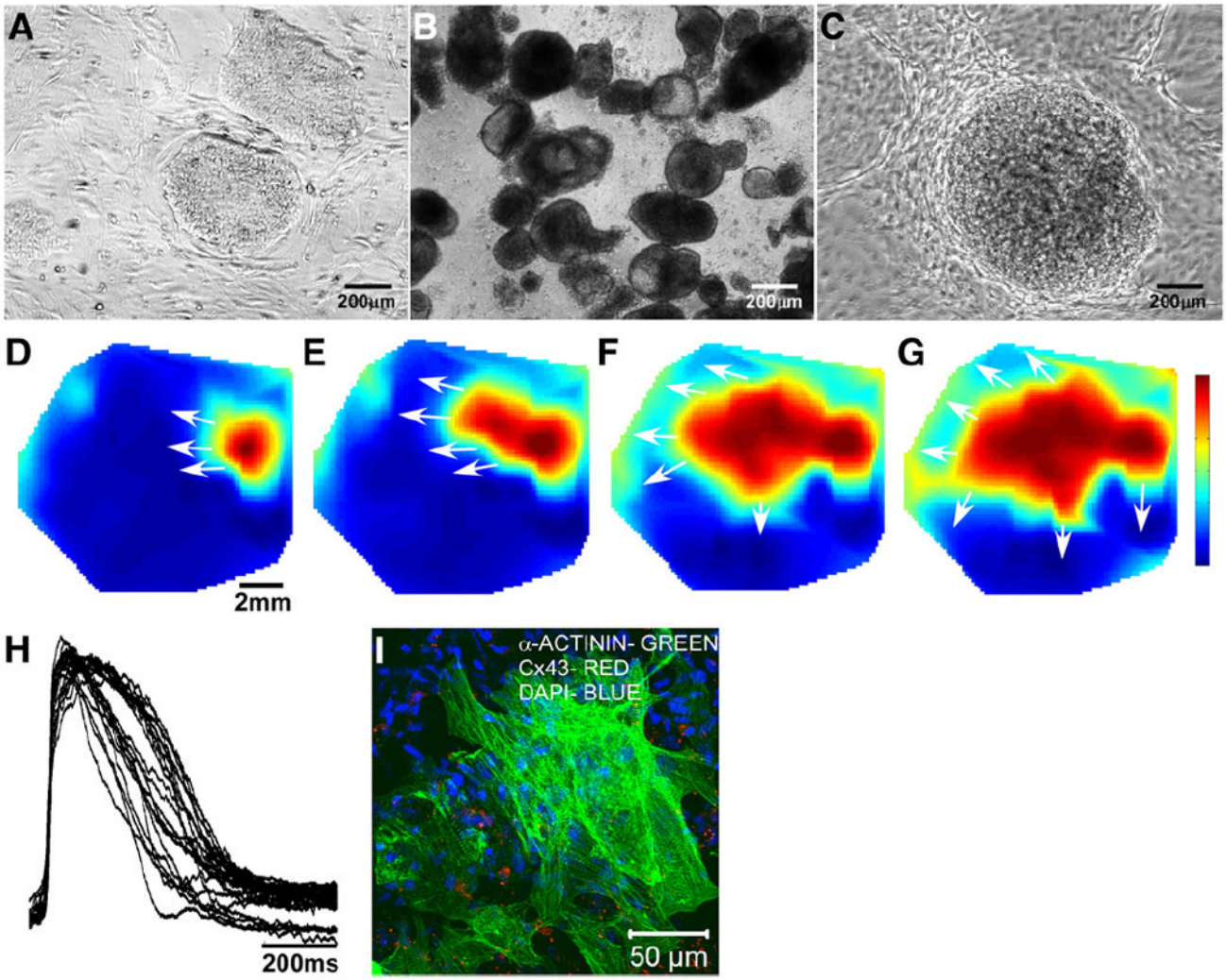

Fig. 2.

hESC-CM differentiation and functional analysis. Phase contrast images show undifferentiated colonies of hESCs grown on MEFs (A), day 7 hEBs grown in suspension (B), and a typical beating hEB imaged on day 18 (C). Voltage maps (D–G, color bar indicates the normalized transmembrane potential: deep red is peak depolarized potential and deep blue is resting potential) starting 30 ms after an electrical stimulus show that monolayers of hESC-CMs can conduct electrical activity across their width of several millimeters. The white arrows display the directions of propagation. Action potentials of hESC-CMs (n=23 representative recording sites) within the monolayer display a sharp upstroke and a several hundred millisecond long duration (H). An immunostained image of α-actinin (green), connexin43 (red), and DAPI (blue) shows large areas of interconnected cardiomyocytes (I) that permit the efficient spread of electrical current.

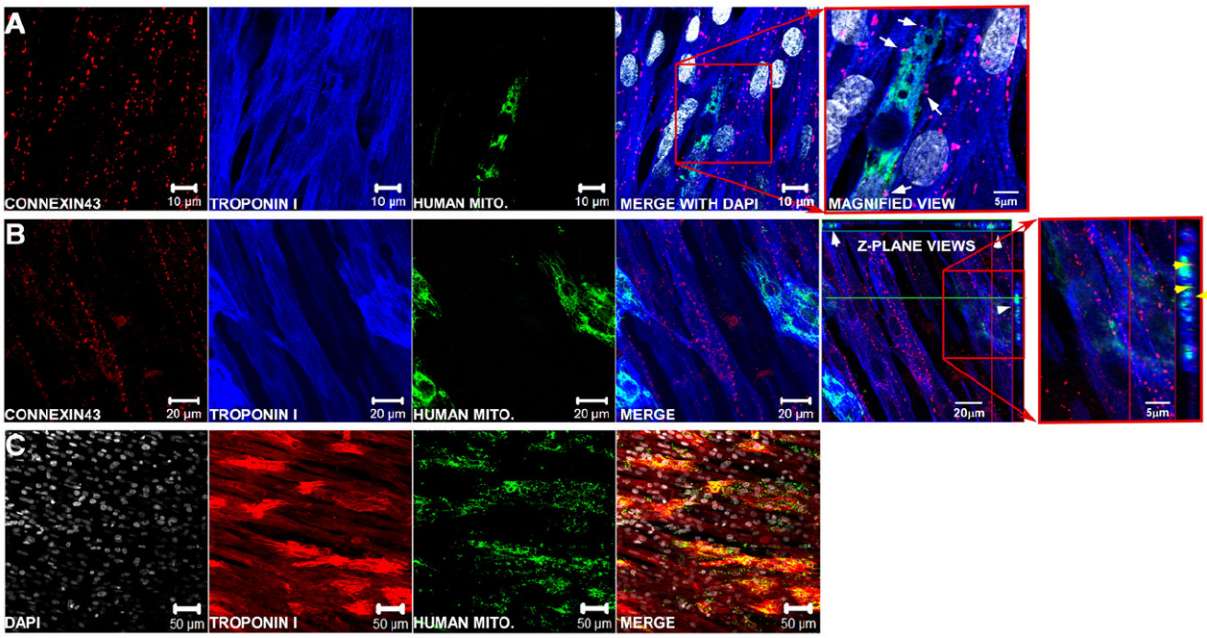

Fig. 3.

Immunolabeled fluorescent images of hESC-CMs incorporated into NRVC monolayers. Monolayers are stained for connexin43 (red), troponin I (blue), and human mitochondrial protein (green) and show that hESC-CMs (green and blue overlay) interact with NRVCs (blue) by either interdigitating laterally with NRVCs (A) or vertically in the z-plane (B). Arrows in A indicate places where hESC-CMs appear to be electrically coupled to NRVCs through connexin43 in a magnified view of the heterocellular contact (selected area denoted by the red box). White arrow heads in the fifth panel from the left in (B) show areas in the x–z and y–z planes (located at the top and right of the image respectively) where hESC-CMs are interacting with NRVCs in the z-direction, and yellow arrow heads in the sixth panel from the left in (B) show areas where hESC-CMs and NRVCs appear to be communicating through gap junctions. A lower magnification image of a monolayer (C) stained for troponin I (red), human mitochondrial protein (green) and DAPI (white) shows the relative distribution and density of hESC-CMs in a typical hESC-CM-supplemented monolayer.

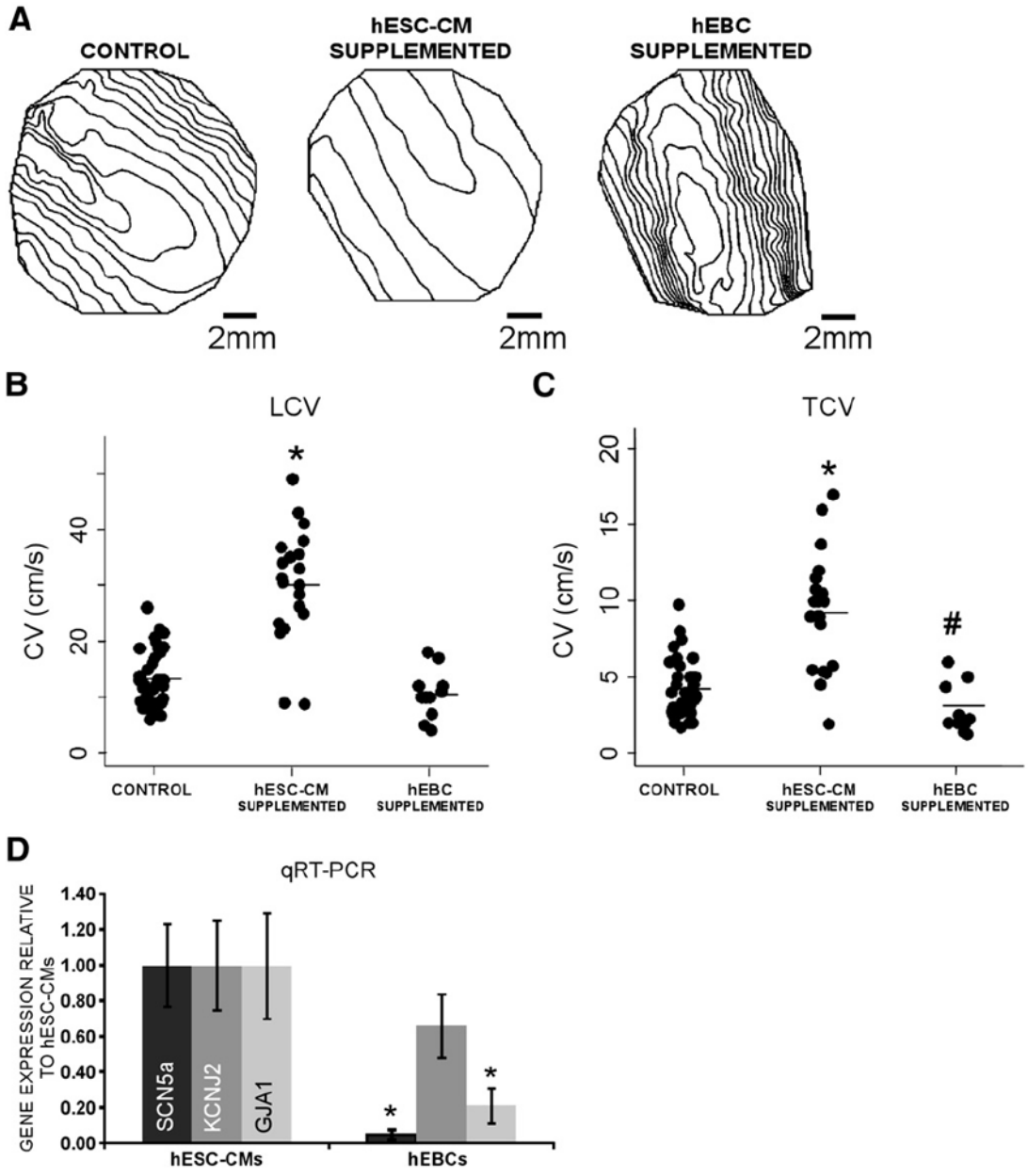

Fig. 4.

Functional improvement of conduction in NRVC monolayers after the addition of hESC-CMs. Isochrone maps (20 ms spacing) obtained at 2 Hz pacing from a representative, control monolayer, hESC-CM supplemented monolayer, and hEBC supplemented monolayer show that the addition of hESC-CMs to NRVC monolayers speeds propagation in the longitudinal and transverse directions (A). Summary dot plots also show that the addition of hESC-CMs significantly elevates longitudinal (LCV, B) and transverse (TCV, C) conduction velocity in NRVC monolayers, whereas the addition of hEBCs decreases LCV and TCV. *Significant difference from control monolayers, $P<0.001$, #Significant difference from control and hESC-CM supplemented monolayers, $P<0.05$. RT-PCR shows that monolayers of hEBCs (n=3) express lower levels of GJA1, SCN5a, and KCNJ2 mRNA than monolayers of hESC-CMs (n=3), which confirms that hESC-CMs, and not hEBCs, have

high gene expression of proteins needed for active electrical signaling (D). *Significant difference from hESC-CMs, $P<0.05$.

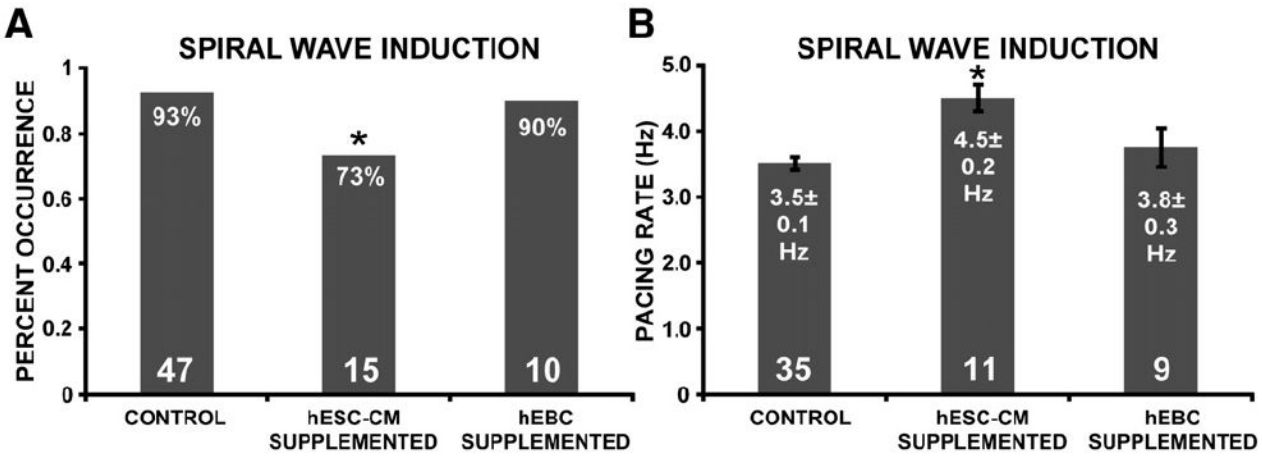

Fig. 5.

Decrease of arrhythmia vulnerability with the addition of hESC-CMs. Reentrant wave occurrence following the addition of hEBCs was not significantly different from reentrant wave occurrence in NRVC monolayers, but was lowered significantly following the addition of hESC-CMs (A). Further, while the pacing rate needed to initiate reentrant waves was significantly higher after the addition of hESC-CMs, the addition of hEBCs had no effect on the initiating pacing rate (B). *Significant difference from control monolayers, $P<0.05$.

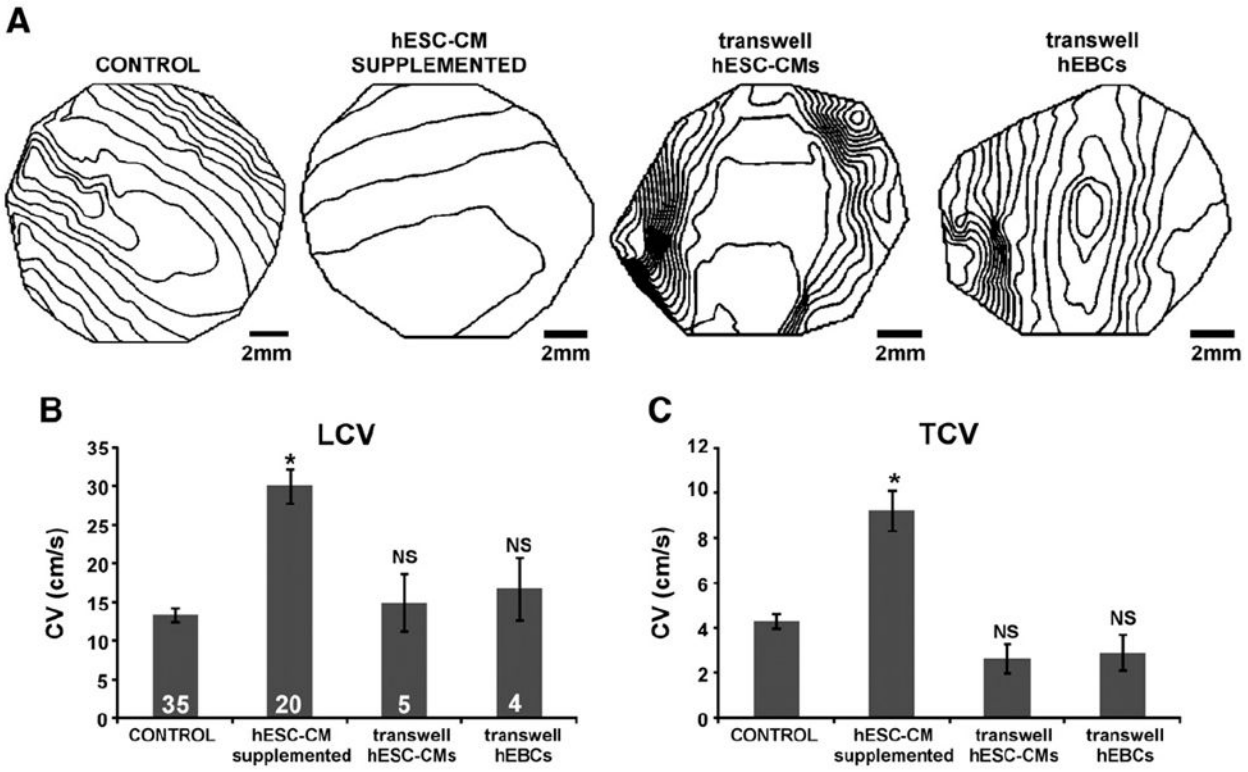

Fig. 6.

Co-culture of hESC-CMs in close apposition to, but not in direct cellular contact with, NRVC monolayers. Isochrone maps (20 ms spacing) paced at 2 Hz from a representative control monolayer, hESC-CM supplemented monolayer, transwell hESC-CM supplemented monolayer, and transwell hEBC supplemented monolayer from the same culture (A). Both the control monolayer and the hESC-CM supplemented monolayer are the same data from Fig. 5. Summary plots of LCV (B) and TCV (C) are shown. *Significant difference from control monolayers, $P<0.05$. ^{NS}No significant difference from control monolayers.

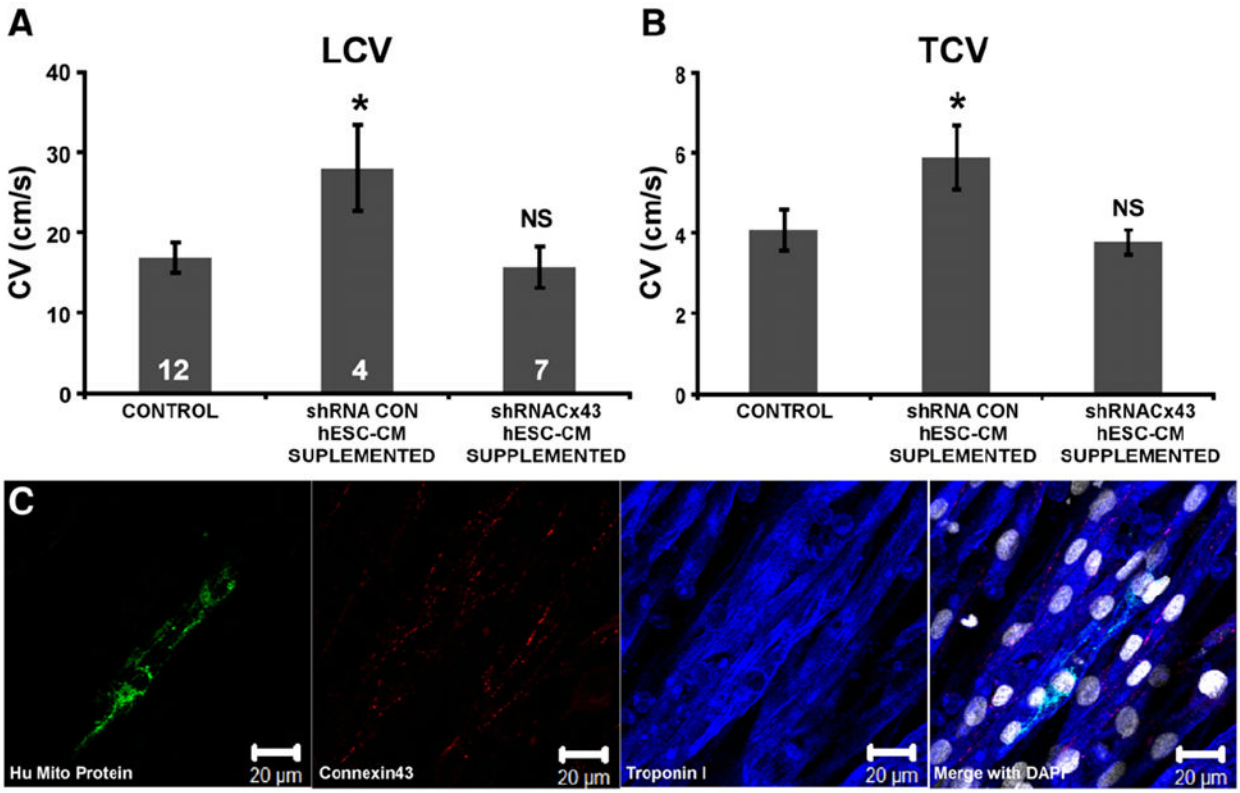

Fig. 7.

Engraftment of connexin43 (Cx43) shRNA hESC-CMs into NRVC monolayers. Summary plots of LCV (B) and TCV (C) show that while engrafted hESC-CMs transduced with scrambled shRNA are capable of improving conduction in NRVC monolayers, hESC-CMs transduced with Cx43 shRNA to prevent electrical coupling to host cardiomyocytes are not. Fluorescence image with immunolabeling for human mitochondrial protein (green), Cx43 (red), α-actinin (blue), and counterstaining with DAPI (white) shows that Cx43 shRNA hESC-CMs survive and engraft into NRVC monolayers (C). *Significant difference from control monolayers, $P<0.05$. ^{NS}No significant difference from control monolayers.